(4)

GL-TR-89-0144 ARC-TR-89-011

Retrieval of Atomic Oxygen and Temperature in the Thermosphere. 1: Feasibility of an Experiment Based on the Spectrally Resolved 147 μm Limb Emission

A. S. Zachor

Atmospheric Radiation Consultants, Inc.
59 High Street
Acton, Massachusetts 01720

10 April 1989

Scientific Report No. 1

GEOPHYSICS LABORATORY
AIR FORCE SYSTEMS COMMAND
UNITED STATES AIR FORCE
HANSCOM AIR FORCE BASE, MASSACHUSETTS 01731-5000

"This technical report has been reviewed and is approved for publication"

(Signature)
RAMESH D. SHARMA
Contract Manager

(Signature)
ANTHONY J. RATKOWSKI
Branch Chief

FOR THE COMMANDER

(Signature)
R. EARL GOOD
Division Director

This report has been reviewed by the ESD Public Affairs Office (PA) and is releasable to the National Technical Information Service (NTIS).

Qualified requestors may obtain additional copies from the Defense Technical Information Center. All others should apply to the National Technical Information Service.

If your address has changed, or if you wish to be removed from the mailing list, or if the addressee is no longer employed by your organization, please notify GL/DAA, Hanscom AFB, MA 01731-5000. This will assist us in maintaining a current mailing list.

Do not return copies of this report unless contractual obligations or notices on a specific document requires that it be returned.

UNCLASSIFIED

SECURITY CLASSIFICATION OF THIS PAGE

REPORT DOCUMENTATION PAGE

1a REPORT SECURITY CLASSIFICATION: UNCLASSIFIED	1b RESTRICTIVE MARKINGS: N/A
2a SECURITY CLASSIFICATION AUTHORITY	3. DISTRIBUTION/AVAILABILITY OF REPORT: Approved for public release; Distribution unlimited
2b DECLASSIFICATION/DOWNGRADING SCHEDULE	
4 PERFORMING ORGANIZATION REPORT NUMBER(S): ARC-TR-89-011	5. MONITORING ORGANIZATION REPORT NUMBER(S): GL-TR-89-0144
6a NAME OF PERFORMING ORGANIZATION: Atmospheric Radiation Consultants, Inc. / 6b. OFFICE SYMBOL (If applicable)	7a. NAME OF MONITORING ORGANIZATION: Geophysics Laboratory
6c. ADDRESS (City, State and ZIP Code): 59 High Street, Acton, Massachusetts 01720	7b. ADDRESS (City, State and ZIP Code): Hanscom AFB, MA 01731-5000
8a NAME OF FUNDING/SPONSORING ORGANIZATION: Geophysics Laboratory / 8b. OFFICE SYMBOL (If applicable): GL/OPB	9. PROCUREMENT INSTRUMENT IDENTIFICATION NUMBER: F19628-87-C-0053
8c ADDRESS (City, State and ZIP Code): Hanscom AFB, MA 01731-5000	10. SOURCE OF FUNDING NOS.

PROGRAM ELEMENT NO.	PROJECT NO.	TASK NO.	WORK UNIT NO.
61101F	ILIR	7B	AA

11 TITLE (Include Security Classification): Retrieval of Atomic Oxygen (Cont.)	
12. PERSONAL AUTHOR(S): A. S. Zachor	
13a. TYPE OF REPORT: Scientific No. 1 / 13b. TIME COVERED: FROM Feb 87 TO Nov 88	14. DATE OF REPORT (Yr., Mo., Day): 1989 April 10 / 15. PAGE COUNT: 40
16 SUPPLEMENTARY NOTATION	

17 COSATI CODES		
FIELD	GROUP	SUB. GR

18. SUBJECT TERMS (Continue on reverse if necessary and identify by block number)

Thermosphere — Limb retrieval
Atomic oxygen density — Remote sensing
Translational temperature — Fabry-Perot

19. ABSTRACT (Continue on reverse if necessary and identify by block number)

The importance of atomic oxygen and translational temperature in mesospheric/thermospheric processes is the motivation to study the feasibility of recovering vertical profiles of the temperature and O-atom density from limb scan data obtained near 147 μm and/or 63 μm wavelength, corresponding to the oxygen atom ground electronic state (OI) transitions. The limb radiance data must be spectrally resolved to recover both temperature and atomic oxygen density if only one of the OI lines is used, which is the approach investigated in this report. We show how the two vertical profiles can be recovered by applying an onion-peeling method to synthetic data. The temperature and O-atom density in each peeled layer are obtained simultaneously by nonlinear least-squares spectrum fitting. Spectral data in the 147 μm line was found to yield reasonably accurate and stable profiles from 300 km down to an altitude between 130 and 90 km, (Cont.)

20 DISTRIBUTION/AVAILABILITY OF ABSTRACT: UNCLASSIFIED/UNLIMITED ☒ SAME AS RPT. ☐ DTIC USERS ☐	21 ABSTRACT SECURITY CLASSIFICATION: Unclassified

22a NAME OF RESPONSIBLE INDIVIDUAL	22b TELEPHONE NUMBER (Include Area Code)	22c. OFFICE SYMBOL
R. D. Sharma	(617) 377-4198	GL/OPB

DD FORM 1473, 83 APR — EDITION OF 1 JAN 73 IS OBSOLETE

UNCLASSIFIED

SECURITY CLASSIFICATION OF THIS PAGE

Block No. 11 (Continued)

...and Temperature in the Thermosphere. 1: Feasibility of an Experiment Based on the Spectrally Resolved 147 μm Limb Emission

Block No. 19 (Continued)

...depending on the noise level and spectral resolution, and gave better results than the stronger 63 μm spectral data below 140 km. We estimate that the S/N and spectral resolution required for successful retrievals could be provided by a confocal Fabry-Perot system operating near 147 μm, although retrievals down to 90 km from data obtained at orbital altitude would require cooled foreoptics roughly a meter in diameter. The forthcoming Part 2 will show that the alternative approach, based on limb radiance data for both OI lines, not spectrally resolved, can be implemented with a much smaller telescope and the conventional parallel design for the Fabry-Perot etalons.

PREFACE

The study described herein was funded by the AFGL FY87 In-House Laboratory Research (ILIR) Program and was sponsored by the Air Force Systems Command through Contract F19628-87-C-0053.

Scientists and engineers who contributed to the reported research are

A. S. Zachor, Atmospheric Radiation Consultants, Inc.
R. D. Sharma, Geophysics Laboratory/OPB
B. K. Yap, Yap Analytics, Inc.
J. P. Riehl, University of Missouri-St. Louis

We gratefully acknowledge the interest and support of Randall Murphy at GL and of the GL Commander, Col. J. R. Johnson. Valuable insights and motivation were provided by A. T. Stair, Jr. when he was Chief Scientist at GL. Howard Smith, when he was at the Naval Research Laboratory, helped us in analyzing Fabry-Perot system capabilities, as did B. K. Yap.

R. D. Sharma, the alternate Laboratory Contract Manager for the study, guided the technical effort and contributed substantially to an expanded version of the present report. The longer version (authored by A. S. Zachor and R. D. Sharma, and having the same title as this report) has been accepted for publication in Planetary and Space Science. The following additional papers and reports were written and/or presented under sponsorship of Contract No. F19628-87-C-0053:

R. D. Sharma and A. S. Zachor, "Signal Requirements for Remote IR Limb Sounding of Atomic Oxygen and Temperature in the Thermosphere," presented at the OSA Topical Meeting on Laser and Optical Remote Sensing, 28 Sept. to 1 Oct. 1987, N. Falmouth, MA.

A. S. Zachor and R. D. Sharma, "Simultaneous Retrieval of Atomic Oxygen and Temperature in the Thermosphere by an IR Limb Scanning Technique," presented at the International Workshop on Remote Sensing Retrieval Methods, 15-18 December 1987, Williamsburg, VA. (Conference proceedings in press).

B. K. Yap, "FIR Fabry-Perot Interferometer Design Tradeoffs," Final Report on Subcontract No. 87-010, Yap Analytics, Inc., 594 Marrett Road, Lexington, MA 02173, 24 March 1989.

J. P. Riehl, "Fabry-Perot Limb Sounding of Atomic Oxygen Density and Temperature," Final Report on Subcontract No. 87-020, Dept. of Chemistry, University of Missouri-St. Louis, St. Louis, MO 63121, 30 January 1989.

1. INTRODUCTION

Atomic oxygen and translational temperature play vital roles in the chemistry and heat balance of the earth's atmosphere above 80 km altitude. However, existing methods for measuring thermospheric profiles of atomic oxygen density and translational temperature have very severe limitations. The paper by Zachor and Sharma (1989), an expanded version of the present report, discusses the chemical processes and cooling mechanisms that involve upper atmospheric atomic oxygen. It also reviews the various techniques that have been used to measure the temperature and O-atom density, and points out their deficiencies.

The present study was undertaken to determine the feasibility of recovering vertical profiles of translational temperature and oxygen atom density from measurements of the limb radiance profile near 147 μm and/or 63 μm wavelength, corresponding to the OI transitions ($^3P_0 \rightarrow {}^3P_1$ and $^3P_1 \rightarrow {}^3P_2$) of the ground electronic state of atomic oxygen. The assumption that the ^3P fine structure levels are in Local Thermodynamic Equilibrium (LTE) with the translational temperature is crucial to the proposed technique, but seems a reasonable one based on the very long radiative lifetimes of the level transitions (see Fig. 1). The principal advantage of the proposed technique over other remote methods (see Zachor and Sharma, 1989) is that no models are needed for relating the observed emission to the oxygen ground-state density.

The sought-after vertical profiles can, in principle, be recovered from a) a pair of limb radiance profiles representing the total (spectrally integrated) apparent intensities of the two OI lines (Sharma, *et al.*, 1988) or b) a spectrally resolved limb radiance profile for just one of the lines. The use of spectrally resolved data implies an instrument with resolving power greater than 2×10^5. This value corresponds to resolved spectral intervals at 63 μm and 147 μm that are comparable to the respective line widths. We estimate that a state-of-the-art Fabry-Perot interferometer based on metal mesh etalon reflectors could achieve resolving power as high as 5×10^5 or possibly 10^6 at these wavelengths. An IR heterodyne system, if one could be designed to operate near 147 μm wavelength, would be more complex, but would easily provide the required high resolving power.

The proposal to remotely sense both temperature and O-atom density using a spaceborne Fabry-Perot sensor system with 63 μm and 147 μm channels was originally put forth by Sharma, *et al.*, (1987, 1988). The 1987 paper outlines a preliminary sensor system concept and describes its critical components. Sharma, *et al.*, (1988) describe the "non-resolved approach" and a method for inverting the dual radiance profiles, and show temperature and O-atom density profiles retrieved from noise-free synthetic data. We have since developed an improved retrieval algorithm, applied it to noise-contaminated synthetic data, and on the basis of the results have evaluated the

feasibility of this approach. The more recent work will be reported in the forthcoming Part 2.

The present report concerns the "spectrally resolved approach". We describe a straightforward retrieval methodology and the characteristics of solutions obtained from synthesized limb spectral data contaminated by noise. Included in the results is a nomograph that defines the combinations of instrument noise-equivalent spectral radiance and resolving power for which the O-atom density and translational temperature can be successfully recovered. These basic data requirements can be translated by the experimentalist to design tradeoffs and system parameters in order to gauge the feasibility of a given sensor concept. In this fashion we evaluate the feasibility of the proposed (Sharma, *et al.*, 1987) Fabry-Perot experiment.

We begin with a summary of the governing radiative transfer equations and a general description of the retrieval method. Section 3 gives some details of the retrieval algorithm. The remaining sections present results and conclusions.

2. RADIATIVE TRANSFER EQUATIONS AND RETRIEVAL METHODOLOGY

The transfer of photon spectral radiance N_υ arising from a single transition at wavenumber υ_0 through a slab of thickness Δz along the line-of-sight can be evaluated by the equation,

$$N_\upsilon(z+\Delta z) = N_\upsilon(z)\exp(-\Delta\tau_\upsilon) + [2c\upsilon_0^2\gamma/(1-\gamma)][1-\exp(-\Delta\tau_\upsilon)], \qquad (1)$$

where c is the speed of light. Equation (1), for appropriately defined γ, is not restricted to the LTE case; see Zachor and Sharma (1985). In the present case LTE is assumed, and γ reduces to

$$\gamma = \exp(-c_2\upsilon_0/T), \qquad (2)$$

where $c_2 = 1.4388\ K/cm^{-1}$ is the second radiation constant and T is the slab temperature. The first factor of the second term in the r.h.s. of equation (1) is then equal to Planck's function evaluated at υ_0, T, while the second factor represents the fraction of radiation escaping the slab. The monochromatic optical thickness of the slab is

$$\Delta\tau_\upsilon = n\,\Delta z\; f(\upsilon-\upsilon_0)\; S(\upsilon_0,T), \qquad (3)$$

where n is the species (O-atom) density, $f(\upsilon)$ is the normalized Voigt shape of the line due to Doppler and collisional broadening, and $S(\upsilon_0,T)$ is the integrated intensity

of the line, given by

$$S(\upsilon_0, T) = (A/8\pi c\upsilon_0^2)[(1-\gamma)/\gamma] g_u \exp(-c_2 E_u/T)/Q(T). \quad (4)$$

Here, A and E_u are the Einstein A-coefficient (s^{-1}) and upper state energy (in cm^{-1}), respectively; they have one of the values given in Fig. 1, depending on whether υ_0 = 68 cm^{-1} (λ_0 = 147 μm) or υ_0 = 158.5 cm^{-1} (λ_0= 63 μm). The statistical weight g_u of the upper state is unity for the 147 μm line and three for the 63 μm line. The partition sum Q(T) is

$$Q(T) = \exp(-c_2 \times 226.5/T) + 3 \exp(-c_2 \times 158.5/T) + 5. \quad (5)$$

These equations, together with an expression for the line shape $f(\upsilon)$, are sufficient for calculating the limb radiance profile spectrally resolved over the 147 μm and 63 μm lines. The Voigt line shape was used in this work, and the effects of both pressure and temperature were included in calculating the collisional (Lorentz) width. For the Lorentz halfwidth at p = 1 atm and T = 296K we used the value 0.329 cm^{-1}. Pressure has an extremely small effect in the inversions to be described because the spectral radiances that are involved correspond to tangent heights greater than 90 km and, more importantly, they have been degraded by an instrument spectral scanning function (see Section 4) that produces approximately the same effect as collisonal broadening corresponding to a fixed, high pressure. The inversion utilizes spectral radiances out to ten Doppler

halfwidths from the line center, but even here the degraded spectral radiance has a very weak dependence on pressure. Pressure broadening would have a significant effect for instrument resolving powers very much higher than were considered in the present study; see Bullitt, *et al.*, (1985). For the purpose of calculating the collisional width we used the pressure profile of the U.S. Standard Atmosphere (1976). Since we ignore the small effect of differences between this reference pressure profile and the "actual" pressure profile, the calculated limb spectral radiance depends solely on the vertical profiles of the O-atom density and the temperature. Hereinafter these profiles will be referred to as [O] and T, both functions of altitude H. Both the monochromatic limb radiance profile and the spectrally resolved limb radiance profile (the monochromatic radiance degraded to the finite resolving power of the instrument) will be denoted $N_\upsilon(H_T)$, where H_T is the tangent height, i.e., the minimum altitude along the line of sight. We will identify a spectral radiance or other spectral quantity as monochromatic or spectrally resolved where necessary.

For later reference we define the monochromatic volume emission rate,

$$\xi_\upsilon([O],T) = A\cdot[O]\cdot f(\upsilon-\upsilon_0) g_u \exp(-c_2E_u/T)/Q(T), \qquad (6)$$

which is the number of photons emitted (in all directions) per unit time per unit wavenumber interval by a unit volume whose

O-atom density and temperature are [O],T. This rate equals $4\pi/\Delta z$ times the last term of equation (1) evaluated in the limit as Δz approaches zero.

The altitude variation of [O] and T from 90 to 300 km altitude is typified by the two models shown in Fig. 2. Figure 3 shows the monochromatic limb radiance profile $N_\upsilon(H_T)$ computed for the 147 μm line using atmospheric model ATOI4 of Fig. 2. The spectrum for H_T = 90 km is shown as a dashed curve for greater clarity. Note that the spectral radiances are plotted in the form log N_υ vs. $(\upsilon-\upsilon_0)^2$, which results in a straight line when N_υ has the Doppler shape. Over the range of abscissa in Fig. 3, which corresponds to distances $\upsilon-\upsilon_0$ less than roughly 2.5 Doppler halfwidths, $f(\upsilon)$ is well-approximated by the Doppler shape. For the largest tangent heights N_υ has very nearly the Doppler shape (same shape as $f(\upsilon)$) because a) the tangent path is optically thin, and b) the temperature is nearly uniform over the path. The tangent path is definitely not optically thin below $H_T \simeq 170$ km.

The retrieval technique, basically an "onion-peeling" method (Goldman and Saunders, 1979), represents the atmosphere as a series of concentric shells, or layers; [O] and T are treated as constant within each layer. The retrieval proceeds downward, layer-by-layer, from some maximum altitude. For the purpose of discussion the sought-after solution may be regarded as the set of [O]s and Ts for each of the layers below this maximum altitude, say, 300 km. The maximum altitude may be the

largest tangent height H_T for which $N_\upsilon(H_T)$ has been measured, or perhaps the largest H_T for which the signal-to-noise of the measurement is deemed adequate. Since the retrieval technique involves a comparison of measured and calculated limb spectral radiances, it is desirable to include in the calculated values the contributions of layers above the maximum altitude. This is accomplished by a starting procedure prior to the onion-peeling process.

The starting procedure exploits the fact that tangent paths above $H_T \simeq 250$ km are optically thin, and that $N_\upsilon(H_T)$ tends to fall off exponentially above this tangent height -- a consequence of the nearly constant temperature and the exponential decrease in [O] with altitude. These properties make it possible to analytically invert an extrapolated limb radiance profile via the Abel transform (see Sharma, *et al.*, 1988). The extrapolated $N_\upsilon(H_T)$ profile corresponding to $H_T > 300$ km, is based on the measured $N_\upsilon(H_T)$ between 260 and 300 km. Specifically, we obtained a closed-form approximation that gives the spectrally resolved volume emission rate at H = 300 km in terms of $N_\upsilon(H_T = 300$ km) and a single radiance scale height derived from the extrapolated $N_\upsilon(H_T)$ profile. This formula is used to recover a 300-km emission rate that corresponds to the same spectral resolution as the measured $N_\upsilon(H_T)$. Then, by using a deconvolution procedure involving the known instrument spectral scanning function, the monochromatic rate $\xi_\upsilon(H = 300$ km) is found. A corresponding predicted volume emission rate $\xi_\upsilon([O],T)$ can be obtained from equation (6) for

given [O],T. By minimizing the least-squares mismatch between the two monochromatic rates, we determine [O] and T at 300 km. These two values define [O] and T at all higher altitudes since T is assumed constant above 300 km, and because [O] vs. H is assumed exponential; under these conditions and for the optically thin case, [O] has the same scale height as $N_\upsilon(H_T)$.

The onion-peeling procedure is pictured in Fig. 4 for a representative layer at some tangent height less than the 300-km maximum altitude. The starting procedure and previous onion-peeling cycles have provided [O] and T for all layers above the one in question. If values of [O] and T are assigned to the layer, one can calculate the limb spectral radiance for the layer tangent height. The solution values of [O] and T are defined as those for which the rms difference between the calculated spectrum N_υ and the corresponding measured spectrum is a minimum. No assumption is made regarding the optical thicknesses of the individual or aggregate peeled layers.

The physical basis of the retrieval method can be defined with the help of equation (6) for $\xi_\upsilon([O],T)$. The (monochromatic) spectral radiance received by a limb-viewing sensor from only the layer at the tangent height is proportional to ξ_υ, evaluated for the layer's [O] and T, times the spectral transmittance of the path between the layer and the sensor. The received single-layer contribution is thus proportional to [O] at all frequencies υ. It depends on

temperature through the line shape function $f(\upsilon)$ and the Boltzmann factor (normalized by $Q(T)$). But since a change in the latter due to a change in temperature is independent of spectral position, the retrieval method relies on $f(\upsilon)$, that is, on Doppler broadening of the line, to distinguish between changes in temperature and O-atom density. Note also that $f(\upsilon)$ decreases with temperature near the line center, i.e., it opposes the change in the Boltzmann factor; throughout the wings it reinforces the Boltzmann factor. This means that there is a range of temperatures for which information on temperature is obtained mostly from the line wings. Any Doppler shift due to platform motion and/or thermospheric wind along the line of sight would be evident in the spectrally calibrated data if it included both sides of the line. The shift is needed to correct the data and could also be used to determine a component of the wind.

Implicit in the onion-peeling nature of the described inversion method is the assumption of a spherically stratified atmosphere. The tomographic, two-dimensional limb reconstruction technique described by Solomon, *et al.*, (1984) could be applied to the problem were it not for the fact that reabsorption is significant; we are not aware of any multidimensional limb reconstruction methods without the optically-thin restriction. A one-dimensional technique that may, in the present application, have an advantage over onion-peeling with respect to noise propagation is briefly described in the Conclusions section.

3. ALGORITHMIC DETAILS

Let $N_{\upsilon i}(CALC)$ and $N_{\upsilon i}(MEAS)$ denote the calculated and measured limb radiance spectra at wavenumber υi for a particular tangent height H_T. Included in the calculated spectrum is the effect of an instrument line shape (ILS), or spectral scanning function, representing the finite spectral resolution of the measurement. Minimizing the sum-square

$$\sum_i [N_{\upsilon i}(CALC) - N_{\upsilon i}(MEAS)]^2 \qquad (7)$$

gives [O] and T at altitude $H = H_T$. We elected to formally minimize the above sum, i.e., to develop coding for two function procedures, X{[O],T} and Y{[O],T}, corresponding to the nonlinear least-square normal equations, symbolically, $X = 0$ and $Y = 0$. In the course of the inversions, these equations are solved using Newton's method.

The atmosphere must be finely divided to obtain reasonable accuracy in the calculated radiances -- we used a vertical thickness of one km for the layers. Generally, reducing the layer thickness, which reduces each layer's contribution to the limb radiance, would tend to increase the potential for instability in the retrieval solution due to noise/error propagation if the solution consists of independent [O],T values for each and every layer. We chose to solve for the [O] and T of just certain layers spaced more than one km apart, and impose the constraint that log[O] and T vary linearly

between these one-km "solution layers". The distance ΔH between solution layers is assigned one of several values depending on the altitude (see Section 4 below). The [O],T values obtained for the maximum altitude in the starting procedure are used as guesses for the first peeled layer; thereafter, guesses are obtained by linearly extrapolating log[O] and T from the previous pair of solution layers. In the event the normal equations have no solution, the guesses are systematically revised.

The profile consisting of connected temperature solutions is smoothed above H = 130 km, where the assigned ΔH is 10 km. Smoothing is performed in each onion peeling cycle, but only for altitudes addressed by the two most recent cycles. Thus, each 10-km interval above H = 130 km is smoothed twice. The smoothing operation eliminates slope discontinuities and reduces propagated noise, both of which can adversely affect stability.

4. CHARACTERISTICS OF THE SOLUTIONS

Retrievals were performed for four cases: In any one case, the synthetic spectral radiance data represents either the 63 μm or 147 μm line, and atmospheric model ATOI2 or ATOI4 (Fig. 2). The resolving power, $R = \upsilon_0/\Delta\upsilon$, where $\Delta\upsilon$ is the full-width-at-half-maximum of the ILS used to degrade the computed monochromatic radiances, is used as the measure of instrument resolution. We used an ILS corresponding to a high-finesse Fabry-Perot system. Over the range of the ILS used for

spectral scanning, it is well approximated by the Cauchy function (Lorentz shape). The noise equivalent spectral radiance (NESR), in units of photons $s^{-1}cm^{-2}sr^{-1}cm$, is the rms of the zero-mean Gaussian noise added to the spectrally degraded radiances. The parameters R and NESR were independently varied over a wide range for each of the four cases. The following discussion emphasizes results obtained using the 147 μm line since those obtained from the stronger 63 μm line were generally inferior below 140 km altitude.

The synthetic 147 μm data for each tangent height consists of 25 samples of the degraded limb spectral radiance over half the line. The spacing of the samples is 8×10^{-5} cm^{-1}. The half-width of the infinitely resolved limb spectral radiance at the higher tangent heights, for model ATOI4, is roughly $2 \times 10^{-4}cm^{-1}$ which is equivalent to 2.5 samples. Note that an instrument half-width equal to this value corresponds to resolving power $68/(4 \times 10^{-4}) = 1.7 \times 10^{5}$. Figure 5 shows (for atmospheric model ATOI4) the monochromatic 147 μm limb spectral radiance and corresponding degraded spectral radiance for two different tangent heights. The two short-dashed curves are N_υ for H_T= 90 km. The narrower of these is the monochromatic N_υ, while the broader one is the degraded N_υ for resolving power 5×10^{5}. The solid curves are similarly defined, except H_T = 290 km. The long-dashed curve is the ILS that was convolved with the monochromatic N_υs to obtain the degraded N_υs. The points in Fig. 5 are samples of the degraded N_υ for H_T= 290 km after addition of noise corresponding to NESR =

2×10^{11} ph $s^{-1}cm^{-2}sr^{-1}cm$. The spectrally degraded data for the higher tangent heights can be said to have the Voigt shape, since the monochromatic N_υ is Voigt (in fact, nearly Doppler) and the ILS is approximately Lorentz. As the figure indicates, the degraded N_υ typically has the long tail of the ILS. Twenty-five samples accommodated the spectral shapes corresponding to the wide range of resolving powers considered. In practice, a sample spacing appropriate to the actual instrument resolving power would be used, and fewer samples would suffice.

The parameter ΔH, defined earlier, is effectively the vertical resolution of the sought-after solution. Initially, retrievals were performed using noise-free, fully resolved ($R = \infty$) data and $\Delta H = 1$ *km* for all altitudes. The retrieval procedure became very unstable below 135 km. At approximately 130 km altitude it failed, i.e., there was no solution to the normal equations. This behavior, which is explained below, gives some insight into the effects of noise. The final version of the retrieval algorithm uses $\Delta H = 10$ km above 130 km, $\Delta H = 4$ km between 130 and 110 km, and $\Delta H = 2$ km below 110 km. These values are adequate to reproduce the true structure of the model [O] and T profiles; they resulted in solution profiles nearly identical to the model profiles over the full range of the limb radiance data (90 to 300 km) for the case $R = \infty$, NESR = 0.

The spacing in tangent height of the data used in the retrievals is the same as the altitude spacing ΔH of the

solution layers. The results reported here correspond to an instantaneous field of view (IFOV) subtending roughly one or two km at the tangent altitude; that is, IFOV smearing effects were not considered. Synthetic data for tangent heights greater than 220 km was generated for two-km H_T intervals and then smoothed to obtain the spectral radiances at 10-km intervals. A given NESR refers to the noise level before smoothing.

The solutions of the nonlinear normal equations inevitably contain some error, even if the data has no noise. Errors in [O],T propagate downward as these values are used to compute the limb spectral radiance N_υ for a lower tangent height and then to retrieve [O] and T for the corresponding altitude. Also, as the retrieval proceeds downward, the actual temperature at the tangent altitude changes, and the sensitivity of N_υ to this temperature is spectrally redistributed. The contribution to N_υ of a unit volume at the tangent altitude depends primarily on the volume's spectrally resolved emission rate ξ_υ, as discussed earlier. Figure 6 shows ξ_υ versus T for $\upsilon = 68$ cm^{-1} (the center of the 147 μm line), and the spectrally nonresolved rate ξ versus T for the 147 μm line. The competing temperature dependencies of the Boltzmann factor and the lineshape function at the line center result in the broad relative maximum in $\xi_{68}(T)$ near T = 500K. For atmospheric model ATOI4 this temperature occurs at approximately 130 km altitude. Thus, N_υ for H_T= 130 km provides temperature information about altitude H = 130 km

principally in the wings of N_υ. But a significant portion of the wing radiance is due to higher layers, which are warmer (have broader ξ_υ due to Doppler broadening) than the 130-km layer. When the onion-peeling procedure has reached $H_T \simeq 130$ km, errors in the computed wing radiance have become significant in comparision to the actual wing radiance from the 130-km layer, resulting in the failure mentioned above. Obviously, noise in the data can be similarly propagated.

It was found that the solutions tend to fall into three categories: For relatively low resolving power and high noise, the retrieval procedure fails at approximately 130 km, but provides an accurate [O] solution and a usable, albeit noisey, temperature solution above this altitude. Over a rather wide range of higher R and lower NESR, the procedure fails at approximately 104 km, but yields accurate [O] and T values for H > 104 km. This is the altitude at which the O-atom density of the models is a maximum. Still higher R and/or lower NESR results in very accurate retrieved profiles for the entire altitude range, 90 to 300 km, of the synthetic data.

The failure of solutions at the altitude of the [O]-profile peak is due to noise propagation in combination with high atmospheric opacity. The transmittance from the tangent point to the exoatmospheric observing instrument, at the center of the 147 μm line, is less than ~ 0.01 for tangent heights less than 104 km. The 63 μm line gave poorer results than the 147 μm line, particularly for the lower altitudes, because of its higher opacity. The 63-μm line-center

transmittance to the tangent point is less than ~ 0.01 for tangent heights less than 120 km.

5. SUMMARY OF RESULTS (for 147 μm Line)

The noise levels and resolving powers corresponding to the three solution categories are defined in Fig. 7. For example, any combination of R and NESR corresponding to a point between the two lowest solid curves results in accurate [O] and T solutions between 300 km altitude and the peak of the [O] profile, near 104 km. Figure 7 is a composite of two such plots obtained separately for the two model atmospheres. Thus, it may not accurately characterize the solution when the true [O] or T profile is very different from those of the models.

The dashed curves in Fig. 7 are lines of constant maximum signal-to-noise, defined as the maximum of the measured $N_\upsilon(H_T)$ for $\upsilon = \upsilon_0 = 68\ cm^{-1}$, divided by the NESR. This is also the required dynamic range of the measurement system. The maximum signal occurs at $H_T \simeq 120$ km for a given resolving power. As R is increased the maximum signal becomes larger, and a given maximum S/N corresponds to larger NESR. The signal-to-noise is considerably lower than the maximum in the wings of the line and at the higher tangent heights, i.e., $N_\upsilon(H_T)$ has a very large range of values. Figure 5 shows that for NESR = 2×10^{11} ph $s^{-1}cm^{-2}sr^{-1}cm$ and $R = 5 \times 10^5$, the lowest S/N in the data is unity, and that the $N_\upsilon(H_T)$ data spans almost four decades.

Figures 8 through 10 show retrieved [O],T profiles representative of the three categories. The point symbols in

Fig. 7 identify the NESRs for Figs. 8-10; the resolving power is 5 x 10^5. Figures 8 and 10 correspond to model ATOI2, representing a cool thermosphere; Fig. 9 corresponds to model ATOI4.

Figures 9 and 10 show clearly that the [O] profile can be recovered to high relative accuracy even when there are large errors, e.g., 100K, in the retrieved temperature profile. This is true at least for the higher altitudes. Generally, the temperature errors decrease from high to low altitude, due to the increase in S/N, provided the solution doesn't fail. When solutions can be obtained down to 90 km (see Fig. 8), the temperature errors at the lower altitudes (90 to ~104 km) become very small, but the errors in [O] tend to be larger below the [O]-atom density peak than above the peak.

6. CONCLUSIONS

The described technique will yield the translational temperature and O-atom density profiles from a limb radiance scan spectrally resolved over the 147 μm line. The level of noise in the data and the spectral resolution have, of course, an effect on the accuracy of the retrieved profiles, but more importantly, they determine the altitude at which the onion-peel retrieval technique becomes unstable. Very accurate profiles can be recovered from ~ 300 km down to 90 km altitude if, for example, the resolving power is 5 x 10^5 and the noise-equivalent spectral radiance is less than 7 x 10^{10} ph $s^{-1}cm^{-2}sr^{-1}cm$. With half this resolving power and ten times

the noise it is possible to recover an accurate O-atom density profile and a rough approximation to the temperature profile above $\sim$130 km altitude. Above 130 km the instrument need only resolve approximately 10 km at the tangent altitude, whereas two-km vertical resolution is required to retrieve the sharp peak of the O-atom density profile near 100 km altitude. The 63 μm line, which is more opaque than the 147 μm line, yields inferior solutions below $\sim$140 km altitude.

A resolving power of 5×10^5 and NESR of 7×10^{10} ph $s^{-1}cm^{-2}sr^{-1}cm$ at wavelength 147 μm work out to a required noise-equivalent radiance of 2×10^{-14} W $cm^{-2}sr^{-1}$. These signal requirements, and the corresponding two-km vertical resolution, were translated to basic design requirements for a Fabry-Perot spectrometer system operating at orbital altitude. It was found that the etalon mesh reflectors, assuming a parallel mesh design, would have to be much larger in size than we believe is practicable. However, a confocal design based on spherical mesh reflectors, which was suggested for the present application by H. A. Smith (personal communication, 1987), can theoretically provide the required performance with an etalon measuring a few centimeters. While the etalon size is more reasonable in the confocal design, it remains to be demonstrated that the theoretical resolving power of 5×10^5 can be achieved in practice. With the confocal design, and a stressed Ge:Ga detector providing a noise equivalent power of 5×10^{-17} W $Hz^{-1/2}$, and a one-Hz noise bandwidth, the system would need cold foreoptics approximately a meter in diameter.

The one-Hz noise bandwidth corresponds to the measurement of $N_\upsilon(H_T)$ at a single combination of υ and H_T. The time available to scan υ and H_T may make it necessary to use multiple detectors and/or a larger collector. Thus, retrievals down to 90 km by the described technique imply a somewhat advanced sensor. A similar system with larger IFOV and cold foreoptics of $\sim$15 cm diameter would allow retrievals from 300 km down to 130 km altitude.

It is likely that the reported signal-to-noise and/or spectral resolution requirements could be reduced somewhat by replacing the onion-peeling procedure by a method that fits, simultaneously, the measured limb spectral radiances for many tangent heights in the data set. This is aptly called the global-fit approach by Carlotti (1988). Chang and Weinreb (1985) refer to it as the Levenberg-Marquardt method after the algorithm they used to effect the nonlinear least-squares fit. Both papers compare results obtained by the global-fit and onion-peeling methods, and conclude that the global technique, which does not tend to propagate noise, yields better solutions. The paper by Carlotti describes a retrieval of stratospheric ozone concentrations by the global-fit approach that required substantial execution time on a Cray computer. This discouraged us from applying the global-fit method to the present problem, which we estimate would require even greater computer resources. Also, we wanted to first compare the spectrally resolved and non-resolved approaches for temperature and O-atom density retrieval, based on onion-peeling. As

pointed out by Chang and Weinreb (1985), the onion-peeling method is valuable as a diagnostic rool; in the present application it helped us recognize a fundamental sensitivity problem near 130 km altitude ($T \simeq 500K$). Onion-peeling combined with global fitting, where the latter is used only for a selected range of altitudes, e.g., 90 to 130 km, could conceivably be used in our application to achieve reduced sensitivity to noise together with reasonable computing time.

Acknowledgments -- We gratefully acknowledge the interest and support of Randall Murphy at the Geophysics Laboratory and of the GL Commander, Col. J. R. Johnson. Valuable insights and motivation were provided by A. T. Stair, Jr. when he was Chief Scientist at GL. Boh Yap of Yap Analytics, Inc. helped us in analyzing Fabry-Perot system capabilities, as did Howard Smith of the Naval Research Laboratory. This project was funded by the AFGL FY87 In-House Laboratory Research (ILIR) Program and was sponsored by the Air Force Systems Command through Air Force Contract No. F19628-87-C-0053.

REFERENCES

Bullitt, M. K., Bakshi, P. M., Picard, R. H. and Sharma, R. D. (1985) Numerical and analytical study of high resolution limb spectral radiance from nonequilibrium atmospheres. *J. Quant. Spectrosc. Radiat. Transfer.* 34, 33.

Carlotti, M. (1988) Global-fit approach to the analysis of limb-scanning atmospheric measurements. *Appl. Optics.* 27, 3250.

Chang, I-Lok and Weinreb, M. P. (1985) Retrieval calculations applied to solar occultation measurements, in *Advances in Remote Sensing Retrieval Methods*, A. Deepak, H. E. Fleming and M. T. Chahine (Eds.), p 149. A. Deepak Publishing, Hampton, VA.

Fischer, C. F. and Saha, H. P. (1983) Multiconfigurational Hartree-Fock results with Breit-Pauli corrections for forbidden transitions in the $2p^4$ configuration. *Phys. Rev. A.* 28, 3169.

Goldman, A. and Saunders, R. S. (1979) Analysis of atmospheric infrared spectra for altitude distribution of atmospheric trace constituents - I: method of analysis. *J. Quant. Spectrosc. Radiat. Transfer.* 21, 155.

Sharma, R. D., Harlow, H. B. and Riehl, J. P. (1988) Determination of atomic oxygen density and temperature of the thermosphere by remote sensing. *Planet. Space Sci.* 36, 531.

Sharma, R. D., Stair, A. T. Jr. and Smith, H. A. (1987) A spaceborne passive infrared experiment for remote sensing of the atomic oxygen density and temperature, and total density in the upper atmosphere. *Adv. Space Res.* 7, 31.

U.S. Standard Atmosphere (1976) National Oceanic and Atmospheric Administration, National Aeronautics and Space Administration, United States Air Force, Washington, DC (October 1976).

Zachor, A. S. and Sharma, R. D. (1985) Retrieval of non-LTE vertical structure from a spectrally resolved infrared limb radiance profile. *J. Geophys. Res.* 90, 467.

Zachor, A. S. and Sharma, R. D. (1989) Retrieval of atomic oxygen and temperature in the thermosphere. 1: Feasibility of an experiment based on the spectrally resolved 147 μm limb emission. Accepted for publication in *Planetary and Space Science*.

FIGURE CAPTIONS

1.) Approximate energy-level diagram for the atomic oxygen OI transitions. Values are given for the energies and for the transition lifetimes and Einstein A-coefficents (after Fischer and Saha, 1983).

2.) Two models for the vertical profiles of atomic oxygen density and translational temperature. They represent a cool thermosphere (ATOI2) and a relatively warm thermosphere (ATOI4).

3.) The spectrally resolved monochromatic limb radiance computed for various tangent heights for the 147 μm line and atmospheric model ATOI4. The abscissa is proportional to the square of distance from the line center.

4.) The geometry of the onion-peel retrieval technique.

5.) Monochromatic and spectrally degraded limb radiance for tangent height 90 km (short-dashed curves) and tangent height 290 km (solid curves). The degraded spectral radiances correspond to resolving power $R = 5 \times 10^5$. The instrument line shape for this R (long-dashed curve) is normalized to fit the radiance scale. The spectral radiances represent the 147 μm line and atmospheric model ATOI4.

6.) The volume emission rate $\xi_{\upsilon}(T)$ evaluated at the center of the 147 μm line (υ = 68 cm^{-1}), and $\xi(T)$ for the 147 μm line. Both are normalized to their values at T = 296K. The spectrally resolved rate ξ_{υ} was calculated from equation (6), in which the Doppler shape was used for $f(\upsilon-\upsilon_0)$.

7.) Noise-equivalent photon spectral radiances (NESR) and resolving powers at λ = 147 μm corresponding to the three solution categories. The dashed curves indicate the corresponding maximum signal-to-noise (required dynamic range).

8.) Actual and retrieved [O] and T profiles for resolving power 5 x 10^5. The NESR is 7 x 10^{10} ph $s^{-1}cm^{-2}sr^{-1}cm$.

9.) Same as Fig. 8, except the NESR is 2 x 10^{11} ph $s^{-1}cm^{-2}sr^{-1}cm$.

10.) Same as Figs. 8 and 9, except the NESR is 5 x 10^{11} ph $s^{-1}cm^{-2}sr^{-1}cm$.

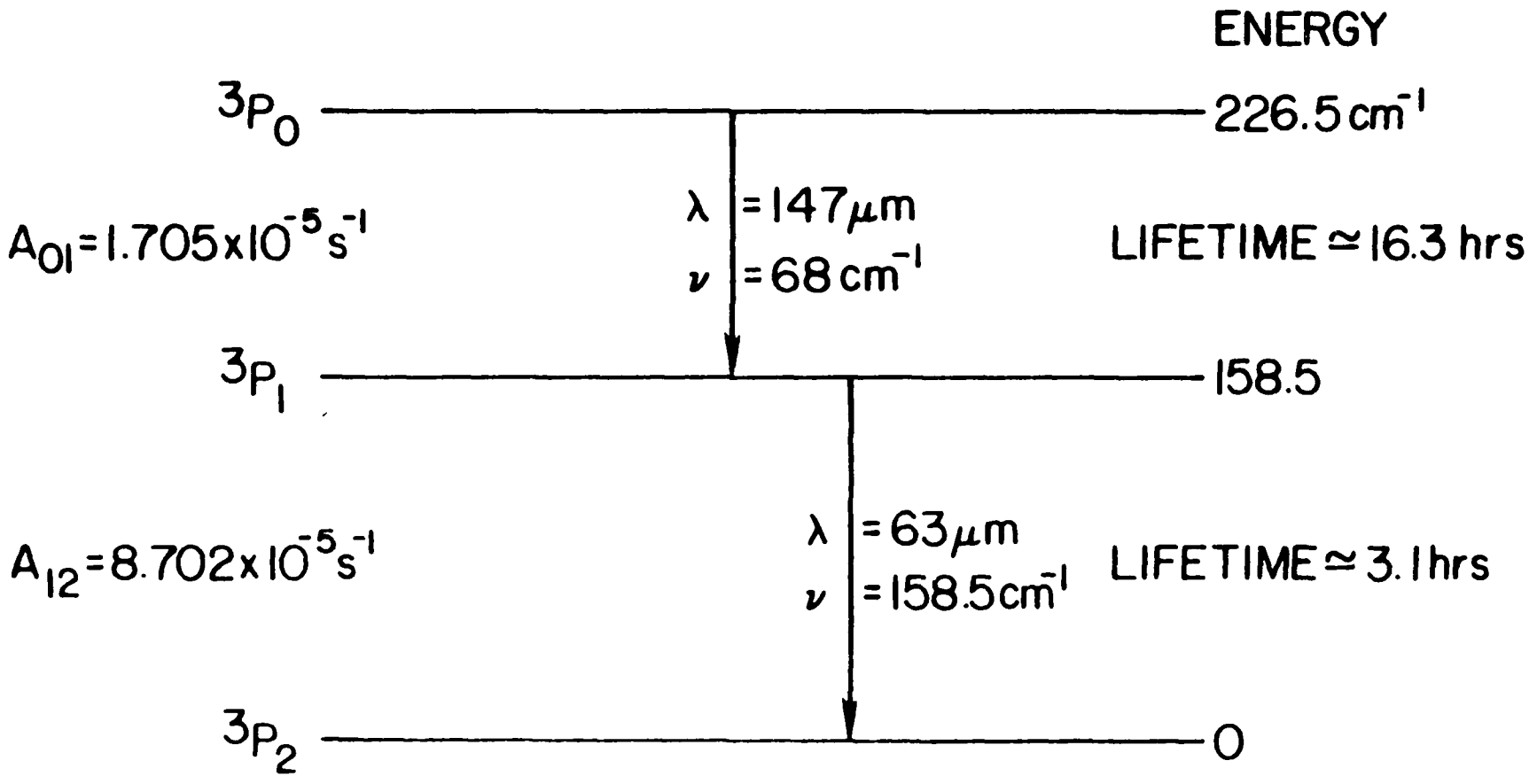
ENERGY
$^3P_0$
226.5 cm^{-1}
$A_{01}=1.705\times10^{-5}s^{-1}$
λ = 147 μm
ν = 68 cm^{-1}
LIFETIME ≃ 16.3 hrs
$^3P_1$
158.5
$A_{12}=8.702\times10^{-5}s^{-1}$
λ = 63 μm
ν = 158.5 cm^{-1}
LIFETIME ≃ 3.1 hrs
$^3P_2$
0

FIGURE 1

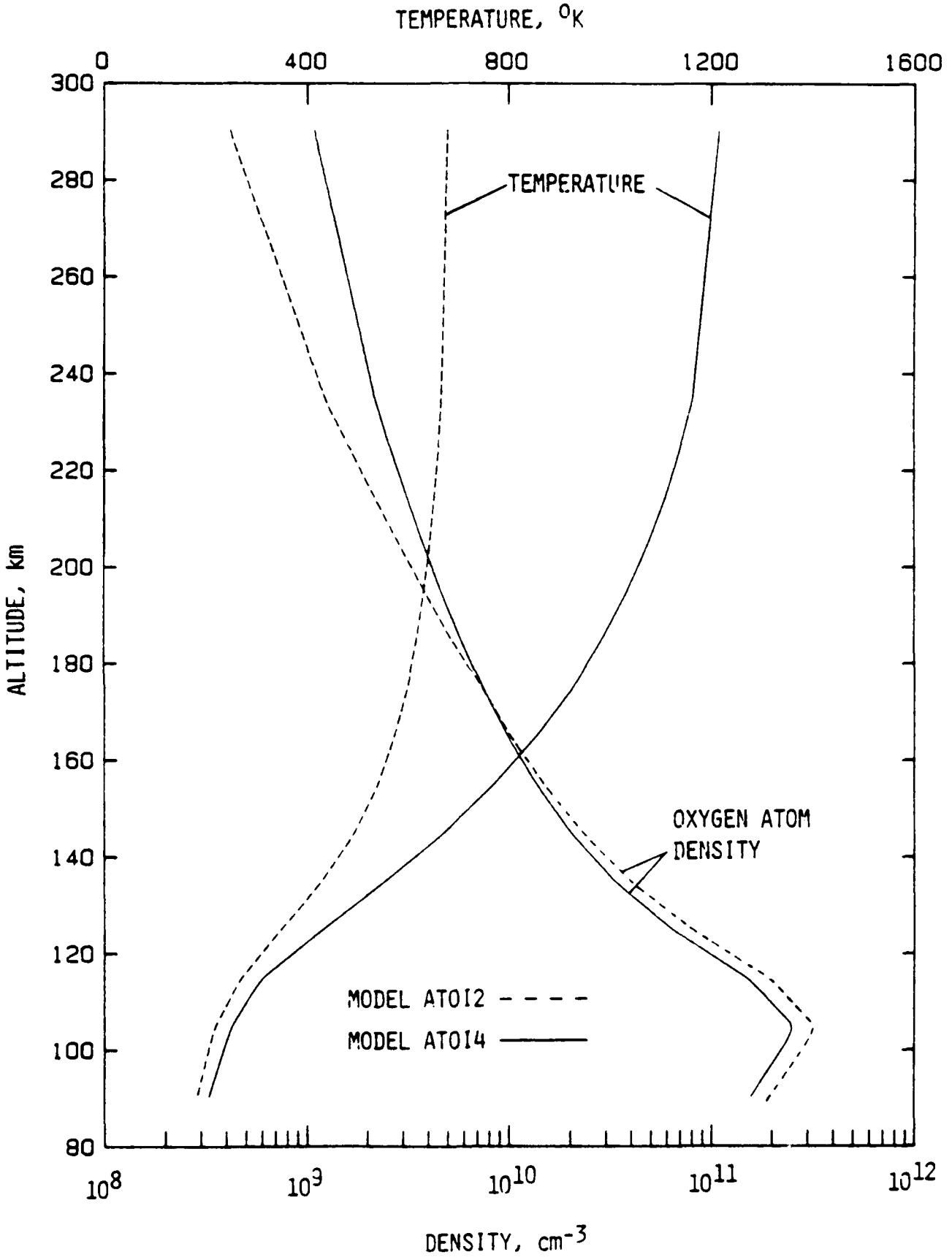
TEMPERATURE, °K
0
400
800
1200
1600
300
280
260
240
220
200
180
160
140
120
100
80
ALTITUDE, km
TEMPERATURE
OXYGEN ATOM DENSITY
MODEL ATOI2 - - - -
MODEL ATOI4 ——
10^8
10^9
10^{10}
10^{11}
10^{12}
DENSITY, cm^{-3}

FIGURE 2

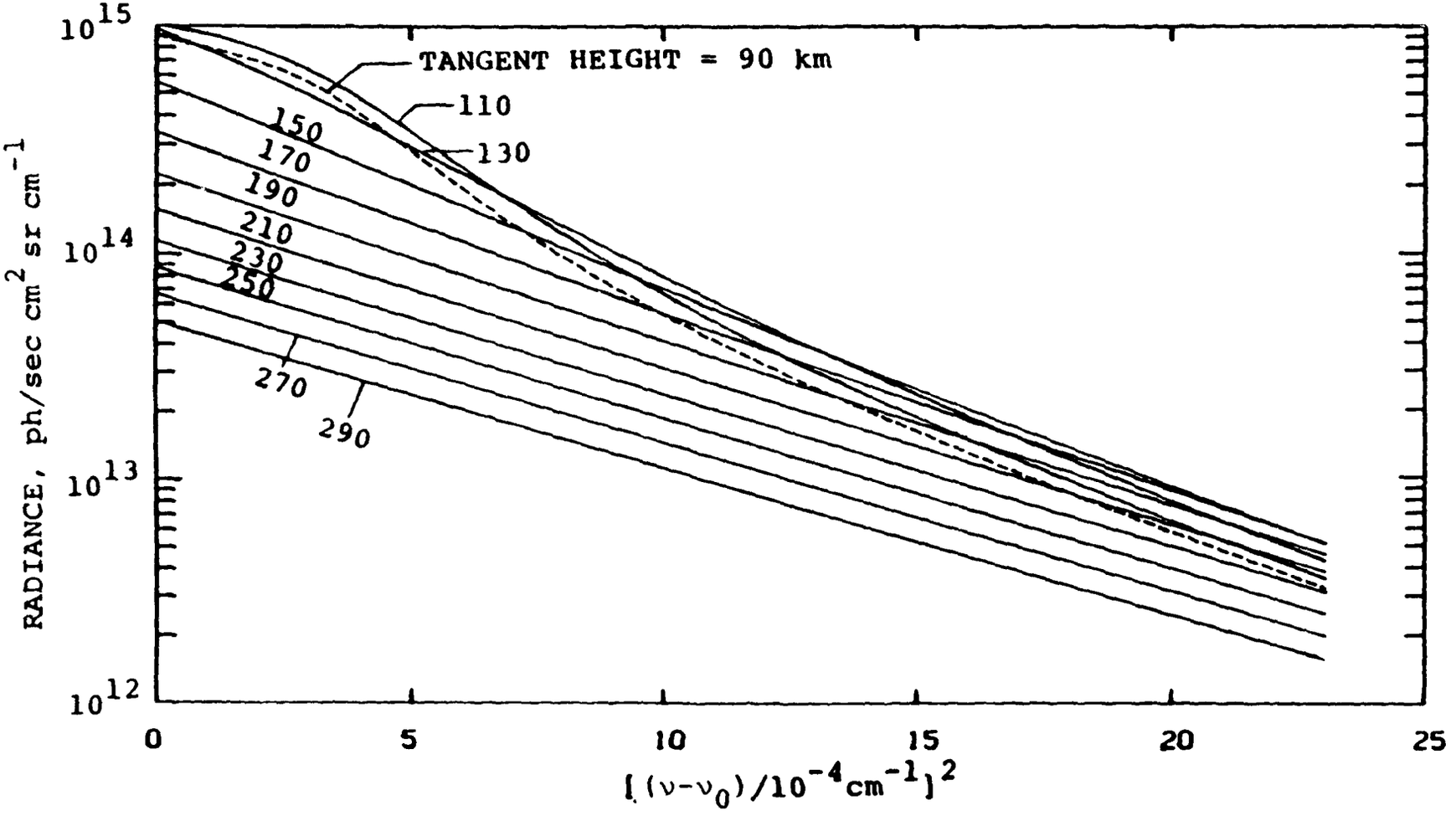
TANGENT HEIGHT = 90 km
110
130
150
170
190
210
230
250
270
290
RADIANCE, ph/sec cm^2 sr cm^{-1}
10^{15}
10^{14}
10^{13}
10^{12}
0
5
10
15
20
25
$[(\nu-\nu_0)/10^{-4}\text{cm}^{-1}]^2$

FIGURE 3

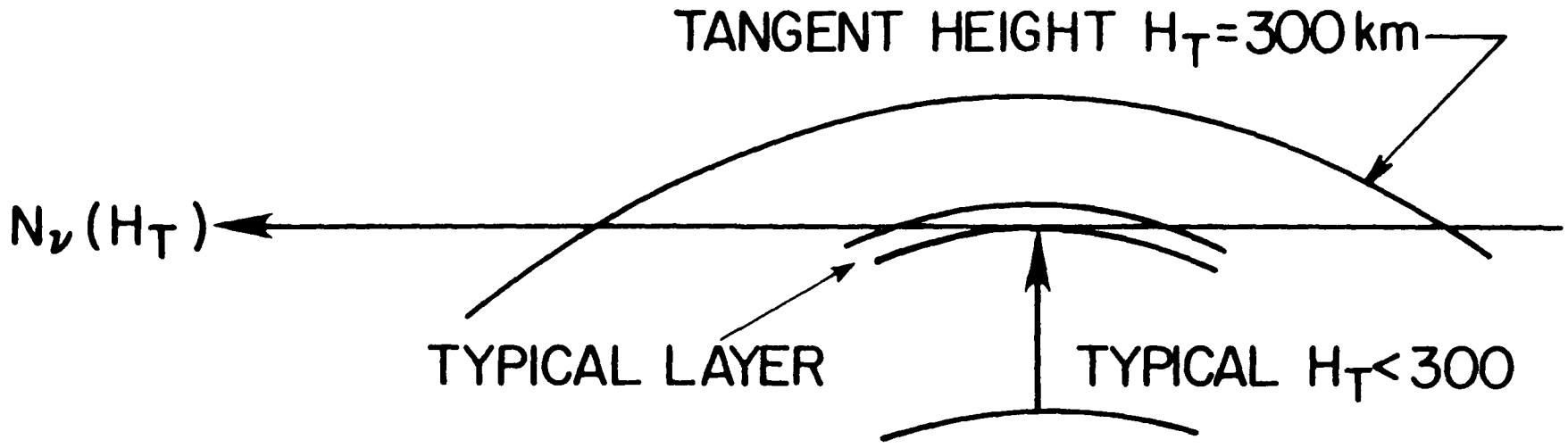

FIGURE 4

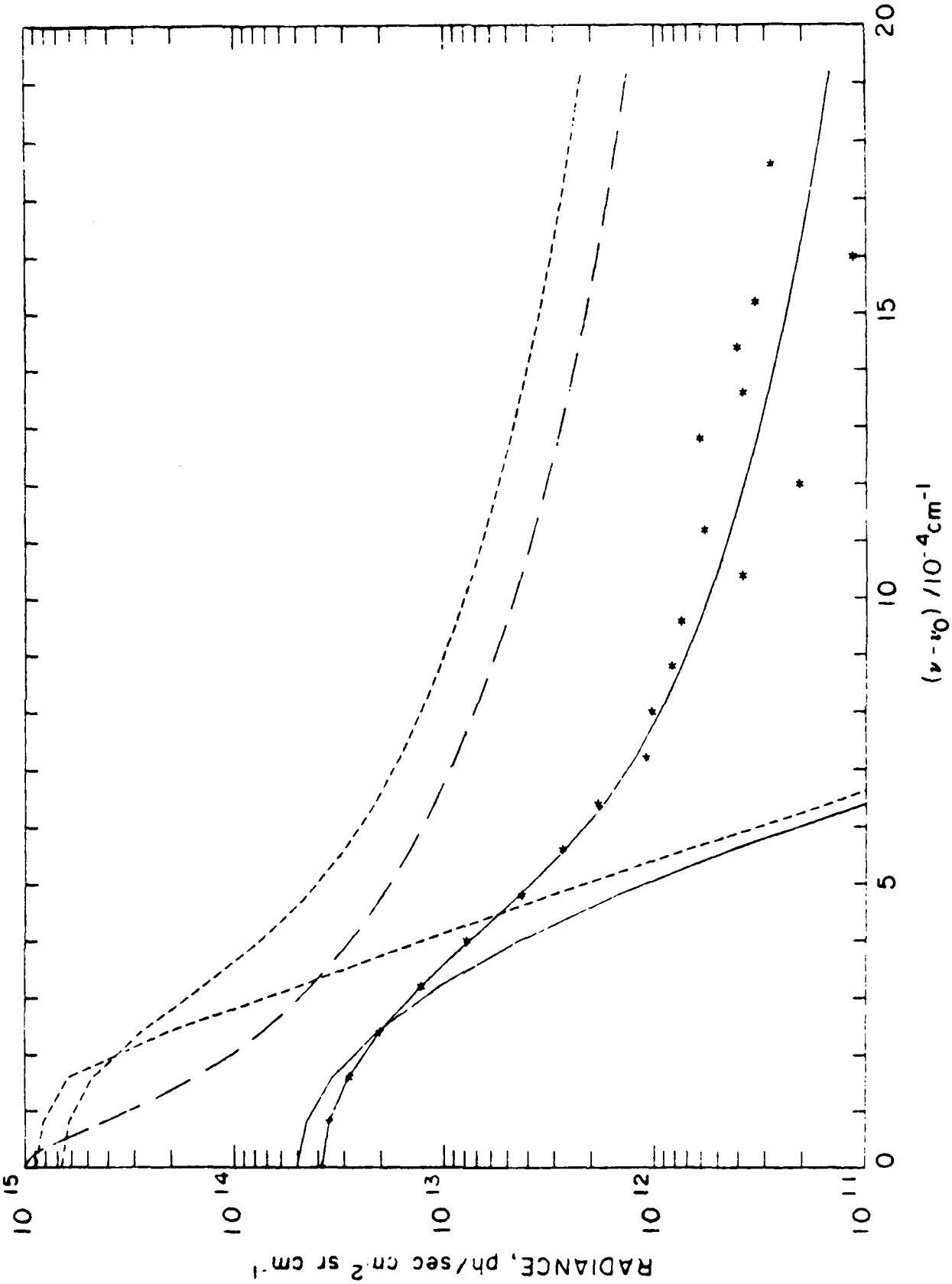
RADIANCE, ph/sec cm^2 sr cm^{-1}
10^{15}
10^{14}
10^{13}
10^{12}
10^{11}
0
5
10
15
20
$(\nu - \nu_0) / 10^{-4} cm^{-1}$

FIGURE 5

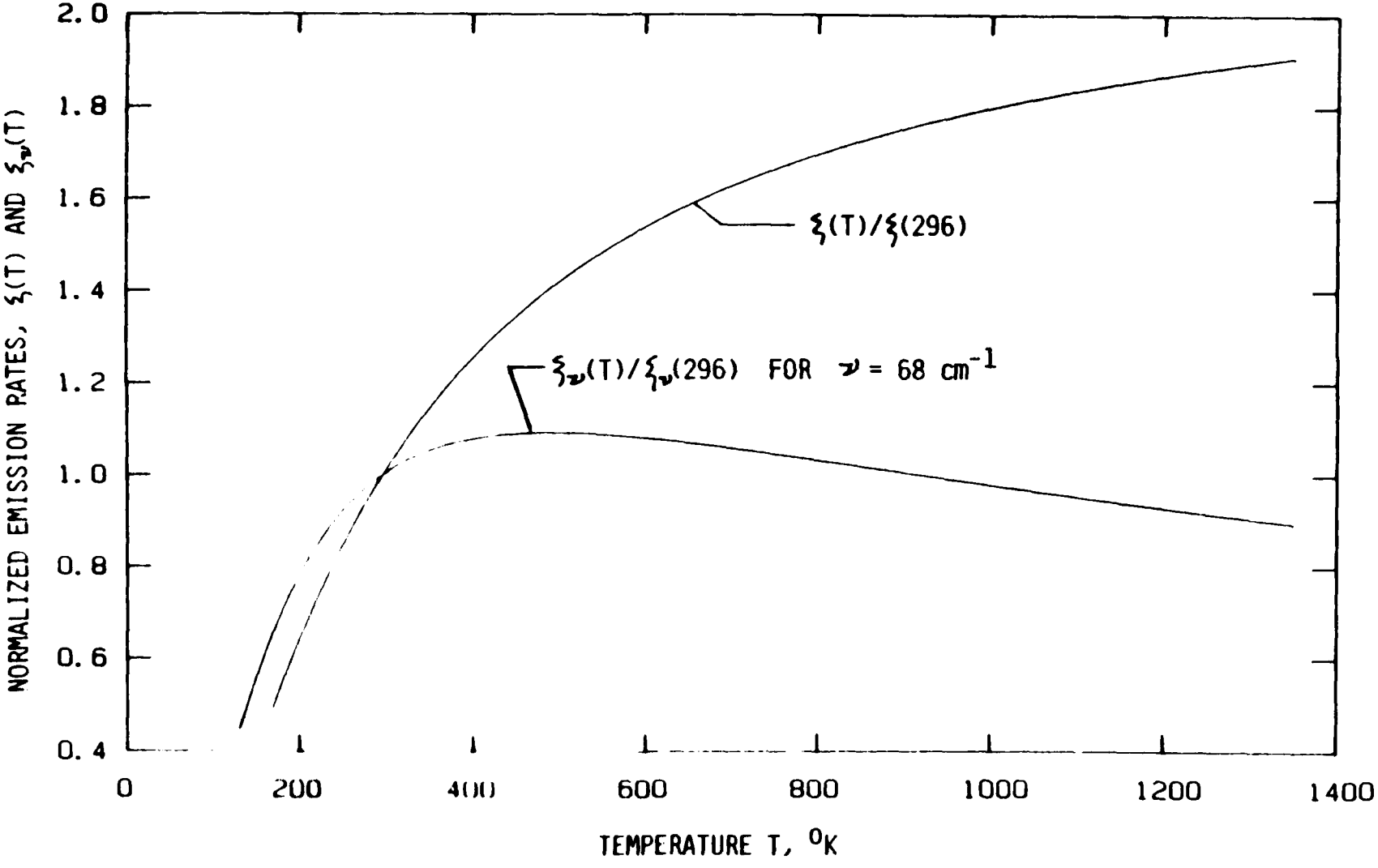
2.0
1.8
1.6
1.4
1.2
1.0
0.8
0.6
0.4
NORMALIZED EMISSION RATES, ξ(T) AND ξν(T)
ξ(T)/ξ(296)
ξν(T)/ξν(296) FOR ν = 68 cm-1
0
200
400
600
800
1000
1200
1400
TEMPERATURE T, °K

FIGURE 6

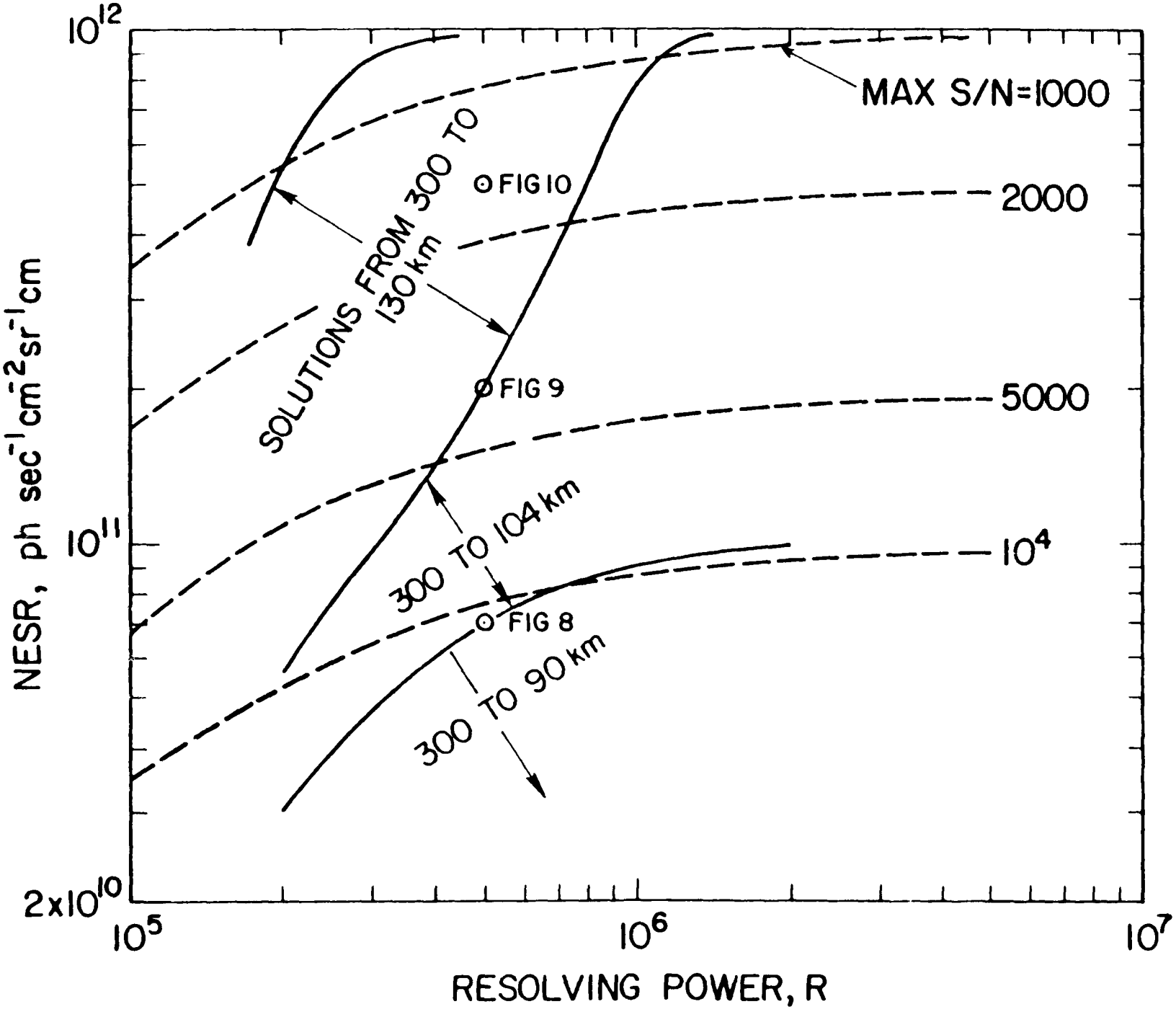
10^{12}
10^{11}
2×10^{10}
10^5
10^6
10^7
NESR, ph $sec^{-1}cm^{-2}sr^{-1}cm$
RESOLVING POWER, R
MAX S/N=1000
2000
5000
10^4
SOLUTIONS FROM 300 TO 130 km
300 TO 104 km
300 TO 90 km
FIG 10
FIG 9
FIG 8

FIGURE 7

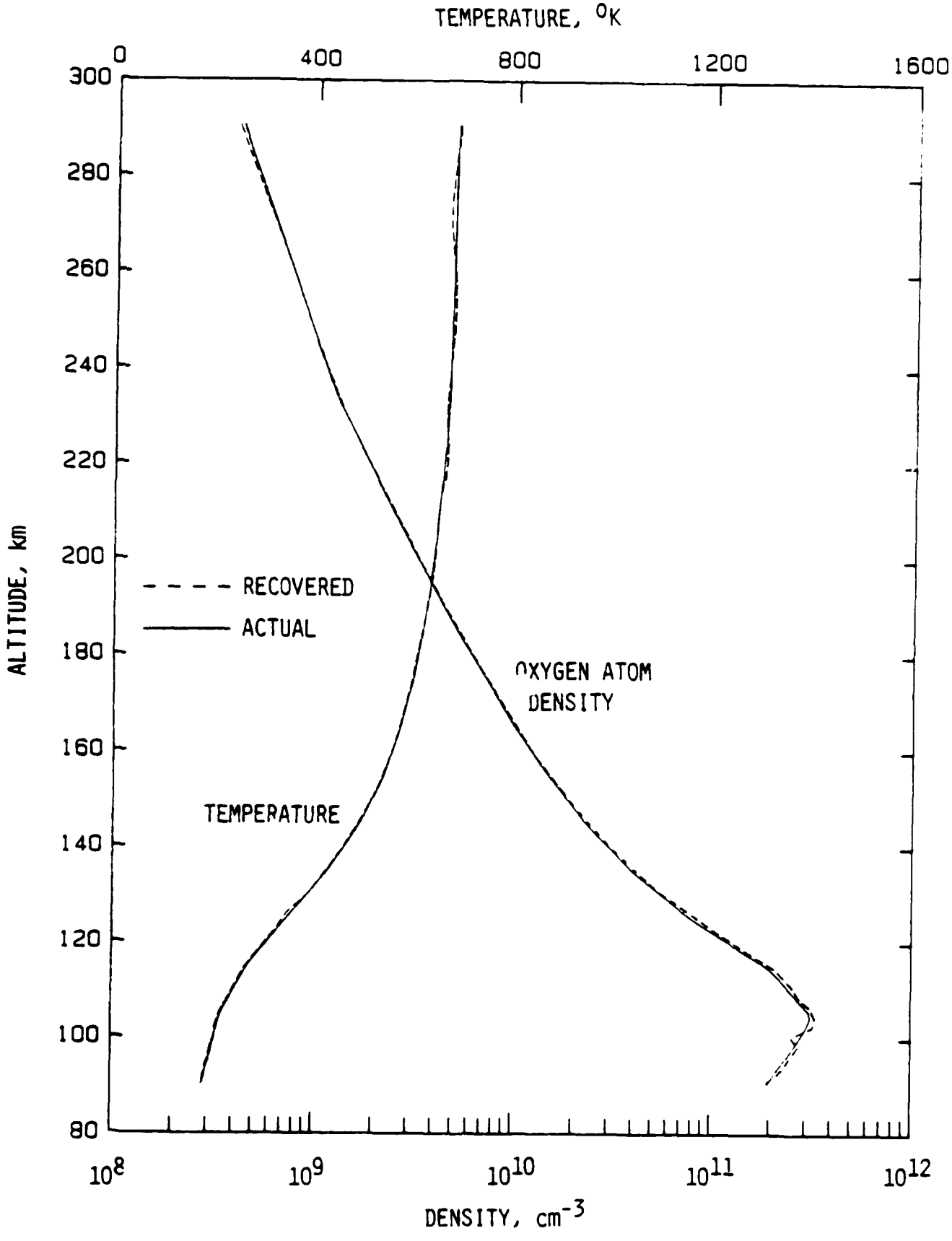
TEMPERATURE, °K
0
400
800
1200
1600
300
280
260
240
220
200
180
160
140
120
100
80
ALTITUDE, km
RECOVERED
ACTUAL
OXYGEN ATOM DENSITY
TEMPERATURE
10^8
10^9
10^{10}
10^{11}
10^{12}
DENSITY, cm^{-3}

FIGURE 8

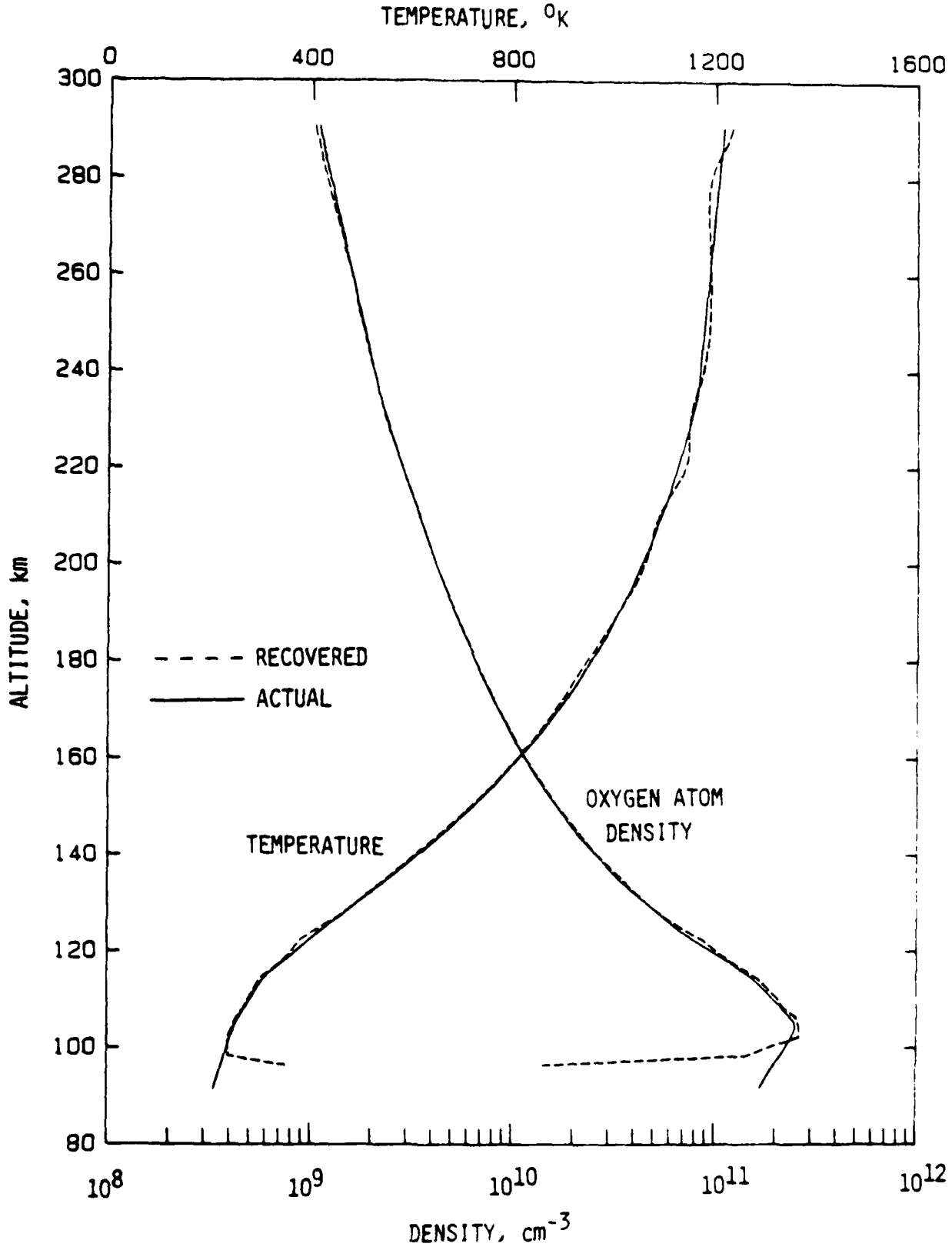
TEMPERATURE, ^{o}K
0
400
800
1200
1600
300
280
260
240
220
200
180
160
140
120
100
80
ALTITUDE, km
RECOVERED
ACTUAL
TEMPERATURE
OXYGEN ATOM
DENSITY
10^{8}
10^{9}
10^{10}
10^{11}
10^{12}
DENSITY, cm^{-3}

FIGURE 9

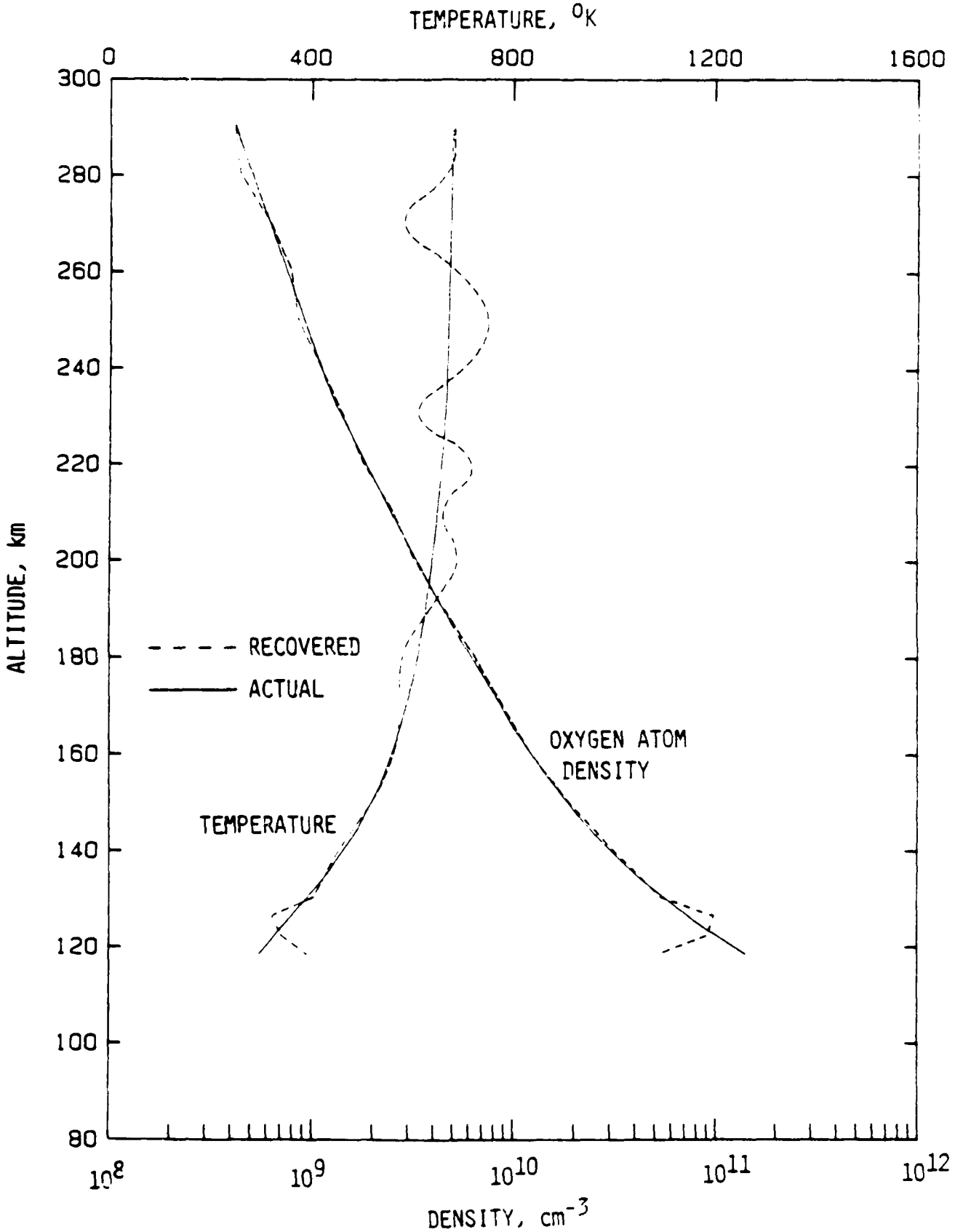
TEMPERATURE, °K
0
400
800
1200
1600
300
280
260
240
220
200
180
160
140
120
100
80
ALTITUDE, km
RECOVERED
ACTUAL
OXYGEN ATOM
DENSITY
TEMPERATURE
10^8
10^9
10^{10}
10^{11}
10^{12}
DENSITY, cm^{-3}

FIGURE 10